JOURNAL OF APPLIED ENGINEERING SCIENCES
ISSN: 2247-3769 / e-ISSN: 2284-7197

VOL. 15(28), ISSUE 2/2025
ART.NO. 453 pp. 195-206

EXPERIMENTAL AND NUMERICAL INVESTIGATION OF MECHANICAL BEHAVIOUR OF EXPANSIVE SOILS UNDER CYCLIC DRYING-WETTING BENEATH PAVEMENTS

M. F. Ahlinhan [a*], O. J. I. Dansou [a], E. C. Adjovi [a], A. Hounsa [a], M. Houata [a]

[a] Research Unit in Geotechnics, Laboratory of Study and Test in Civil Engineering (L2EGC), National High School of Public Works (ENSTP), department of civil engineering, National University of Sciences, Technologies, Engineering and Mathematics (UNSTIM), Abomey 2282 Goho, Department of Zou, Republic of Benin.
E-mails: *ahlinhan@yahoo.fr, danorphe@yahoo.fr, adjed2012@gmail.com, ange2000aurelecc@gmail.com, moisehouata999@gmail.com

Received: 13.09.2025 / Accepted: 15.10.2025 / Revised: 10.11.2025 / Available online: 15.12.2025

DOI: 10.2478/jaes-2025-0023

KEY WORDS: Expansive soils, cyclic drying-wetting, shear, consolidation behaviour, Pavement, FEM.

ABSTRACT:

Expansive soils exhibit considerable volumes changes in response to humidity fluctuations, swelling upon water absorption and shrinkage during desiccation. This recurrent volumetric instability can induce differential settlements, often resulting in structural distress such as cracking in lightly loaded constructions. This study aims to analyse the behaviour of expansive soils under shrink-swell cycles by means of direct shear tests, oedometer tests and finite elements analysis. Hereby, number of cyclic drying-wetting of N=0, N=1, N=2, N=3, N=4, N=5, N=6, N=7, N=8 was investigated for more 200 undisturbed expansive soils from 6 locations in the study area. The soil samples exhibited a pronounced volumetric expansion of approximately 10% during the first two drying–wetting cycles. Beyond this stage, the swelling amplitude progressively diminished with each subsequent cycle, stabilizing at about 1% by the eighth cycle (N = 8). However, the shrink magnitude increased approximately from 10% to 50% as the number of swell-shrink increases. extent of cracking progressively increased with the number of swell-shrink cycles, resulting in an enlargement of the mesopore volume within the samples. Results from the direct shear tests performed under unconsolidated–undrained (UU) conditions showed that both the angle of internal friction and the cohesion underwent a pronounced reduction during the first two cycles. Thereafter, these parameters converged toward residual values corresponding to approximately 30% and 35% of their initial internal friction angle and cohesion, respectively. Exponential decay functions are derived from the test data, that describe the degradation of the shear strength, the angle of internal friction and the cohesion with increasing numbers of drying–wetting cycles. Furthermore, a finite element model has been developed by means of the software Abaqus for analysing the response of pavement resting on expansive soil under to repeated shrink-swell. The finite elements model has been validated with the in-situ results of falling weight deflectometer. The numerical results demonstrated that the pavement deflection and shear strain increase with increasing cyclic drying-wetting. As a result, cracks can occur in the pavement and compromising the serviceability limit state and the integrity of the pavement structure.

GRAPHICAL ABSTRACT:

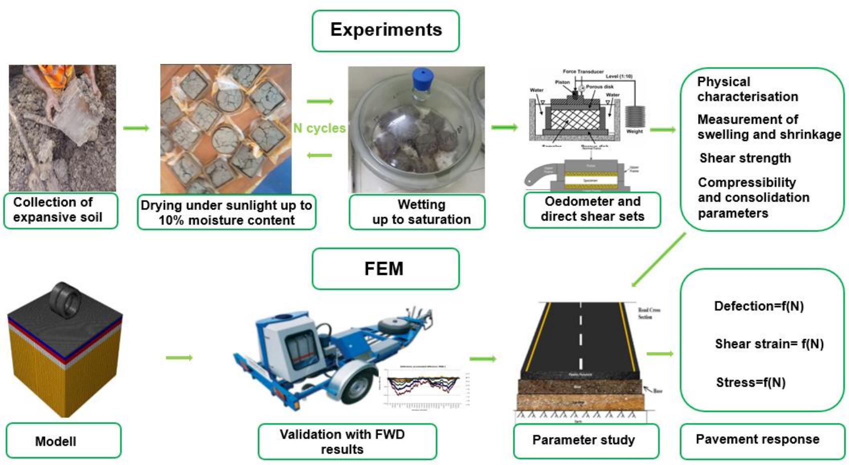

1. INTRODUCTION

Expansive soils are characterized by considerable volumes changes (increase or decrease) in response to humidity fluctuations (Ahlinhan et al., 2025). Expansive soils are widespread globally and represent a major concern due to the considerable structural damage they can cause. The primary mechanism behind this damage is the swell–shrink behaviour of expansive clays.

In regions characterized by pronounced seasonal fluctuations in moisture and precipitation (such as tropical, arid, and semi-arid zones) lightweight structures, pavements, and highways founded on expansive soils are routinely exposed to recurrent swelling and shrinkage cycles. Specifically in tropical zones, expansive soils beneath lightly loaded structures such as light buildings and pavement systems typically undergo two shrink-swell cycles per year due to seasonal climatic variations characterized by two alternating dry and rainy periods. The phenomenon of shrink-swell is linked to volume changes which lead to ground movement and results in undesirable cracking and fatigue to structures.

Damage to structures on expansive soils incurs annual costs of approximately £150 million in the UK, $1 billion in the US, and several billion globally (Gourley et al., 1994; Estabragh et al., 2018). The Association of British Insurers evaluated the annual cost of subsidence associated with shrink-swell behaviour exceeds £400 million for the insurance industry (Driscol and Crilly, 2000; Estabragh et al., 2018).

Swelling and shrinkage magnitude is a critical parameter in ensuring the safety and reliability of foundation design and analysis (Ahlinhan et al., 2025; Chen, 1975; Nelson and Miller, 1992).

Swelling in expansive soils typically occurs in three distinct phases: the initial phase, the second phase, and the no-swelling phase (Day, 1999; Estabragh et al., 2015). The initial phase is characterized by a rapid rate of volume increase during which the fissures formed during drying are quickly reclosed upon subsequent wetting. The second phase is characterized by the progressive closure of micro-cracks and the dissipation of entrapped air. During the third phase, no further volumetric change or variation in void ratio is observed. Likewise, the drying process of soils progresses through three phases: structural shrinkage, normal or primary shrinkage, and residual shrinkage (Haines 1923). These phases are governed by the degree of moisture loss and are influenced by the soil's structure and, crucially, the quantity of interparticle bonding that resist deformation (Bell, 2000; Popescu, 1979). During the structural and residual shrinkage phases, the decrease in soil volume is smaller than the corresponding volume of water expelled. However, in the normal shrinkage phase, the change in soil volume closely matches the volume of water lost. Haines (1923) observed that at the shrinkage limit or the onset of the residual phase, the soil volume decreases at a slower rate than water loss, as soil particles begin to come into contact. Once particle-to-particle contact becomes fully established, additional shrinkage ceases despite the continued loss of water.

Expansive clay soils, typically rich in smectite, montmorillonite, or swelling clay minerals, exhibit significant shrinkage and swelling in response to fluctuations in moisture content. If not properly managed, these volumetric changes can cause considerable deterioration and damage to lightly loaded structures. Expansive clay soils are prevalent over wide areas worldwide, and it poses risks to lightly loaded structures, as it is prone to differential deformations primarily driven by fluctuations in moisture content. Climatic conditions can exert a substantial influence on soil moisture variations, particularly through evapotranspiration during dry seasons and infiltration during periods of rainfall. In this context, it is essential to examine the effects of cyclic shrink-swell processes on the mechanical behaviour of expansive soils.

Ahlinhan et al., (2025) investigated the physical and mechanical behaviour of expansive soils subjected to up to eight shrink-swell cycles. The soils were gathered from the La Lama depression in the southern region of the Republic of Benin. Results from direct shear and consolidation tests indicated that the majority of the reduction in shear strength occurred within the first three drying-wetting cycles. Specifically, the internal angle of friction decreased up to 30% of the initial internal angle of friction, and the cohesion dropped by about 35% of the initial cohesion under unconsolidated undrained conditions. However, this study did not examine the extent of swelling and shrinkage with increasing number of drying-wetting cycles, nor did it address the performance of pavement systems constructed on expansive soils under such cyclic conditions.

Chabi et al., (2025) investigated the impact of cyclic wetting-drying on the shear strength, compressibility, and consolidation behaviour of expansive soils in the Lama depression, Republic of Benin. Direct shear tests and oedometer were carried out on expansive soil samples underwent up to three wetting-drying cycles. The results showed a general decrease in unconsolidated and undrained shear strength with increasing cycles, indicating degradation of the soil matrix and the development of significant cracking. However, the study was limited to a single site and a maximum of three cycles.

Gbaffonou et al., (2021) and Gbaffonou (2022) conducted oedometer tests on expansive soil subjected to four cycles of wetting-drying. The results indicated that with increasing number of cycles, the compressibility index increased, while the swelling index decreased. Additionally, the soil's permeability exhibited a rising trend with additional cycles. However, Abbas et al., (2023) observed that cyclic wetting-drying under constant stress conditions led to cumulative shrinkage and a decrease in saturated hydraulic conductivity. Under constant volume conditions, the cyclic process resulted in a reduction in swell pressure, with negligible effect on saturated hydraulic conductivity. These contrasting behaviours suggest that the evolution of hydraulic conductivity in expansive soils under repeated drying-wetting is highly dependent on the mineralogical composition of the clay fracti and the imposed boundary conditions, such as surcharge and volume constraints.

Md et al., (2016) investigated the shear strength variation in residual soils under drying–wetting cycles. For that, triaxial tests were conducted on soil samples retrieved from various locations in the Kaiping region, Guangdong Province, China, under consolidated drained conditions. The experimental results demonstrated that the stress-strain response exhibited pronounced strain-hardening behaviour. With increasing net normal stress, both the deviatoric stress and the initial tangent stiffness increased, and the volumetric response became increasingly contractive. Conversely, an increase in the number of drying-wetting cycles led to a progressive reduction in deviatoric stress and initial stiffness. Furthermore, both the effective cohesion and internal friction angle decreased with successive cycles, with cohesion exhibiting a higher rate of degradation compared to the friction angle. The authors proposed that the evolution of these shear strength parameters with respect to the number of drying-wetting cycles can be accurately described by exponential decay functions. Estabragh et al., (2015) conducted an experimental study to evaluate the impact of cyclic wetting-drying on the hydro-mechanical response of an expansive soil, consisting of a bentonite–kaolin mixture (classified as CH), using a modified oedometer apparatus under various constant loading conditions. The results demonstrated that, upon reaching a quasi-equilibrium state, the volumetric deformation response of the soil became reversible, with successive wetting and drying cycles converging toward a stable, S-shaped hysteresis loop. Furthermore, specimens prepared with a reduced initial water content (highlighting the sensitivity of expansive soils to initial suction and moisture conditions.

Louati et al., (2018) analysed the impact of repeated wetting-drying and crack development on the hydraulic conductivity of compacted clayey soils. Their findings revealed a strong correlation between predicted and experimentally measured saturated hydraulic conductivity values. The study further demonstrated that the formation of desiccation cracks significantly increased the soil's permeability, up to a critical threshold. Beyond this point, particularly after seven wetting-drying cycles, the influence of the initial compaction density on hydraulic conductivity became negligible.

Basma et al., (1996) investigated the cyclic swelling-shrinkage behaviour of natural expansive clays and established that such cyclic processes have a pronounced effect on the expansive characteristics of these soils. Their study reported a progressive reduction in swelling capacity and water absorption when the soils were subjected to repeated wetting and partial drying. However, when soils experienced full shrinkage between cycles, an increase in the swelling potential was noted. In both scenarios, the soil behaviour tended toward equilibrium after several cycles. With continued cycling, progressive breakdown of macro-aggregates and increased disorientation of the soil fabric were observed. By approximately the fifth cycle, the soil structure approached a fully disoriented state, beyond which further changes in expansibility became negligible.

The review of the aforementioned studies highlights that the shrink-swell behaviour of expansive soils under seasonal moisture variations is governed by a complex interplay of factors, including the type and quantity of clay minerals, specific surface area, the proportion of non-expansive constituents, initial water content, and applied surcharge. Cyclic wetting and drying notably affect both the physical and mechanical properties of these soils. However, the majority of previous investigations into the effects of alternating drying–wetting cycles have focused primarily on natural expansive soils, artificially modified soils (e.g., those treated with fly ash, cement, lime, or organic polymers), or reconstituted soils designed for slope stability assessments and ground improvement applications. Moreover, the magnitude of swelling and shrinkage, and the response of pavement system on expansive soils under repeated shrink-swell conditions are not yet well understood. Therefore, this study aims to investigate physical and mechanical response of expansive soils under repeated drying-wetting conditions beneath pavement system. For that experimental and numerical methods have been used.

2. MATERIAL AND METHODS

Material

First, on-site visits were conducted for identifying the locations where shrink-swell effects are most evident, and significant damages and cracks were observed in buildings and pavements. These locations are showed in the study area (Figure 1). Table 1 shows the geographical coordinates of the sampling locations in the study area.

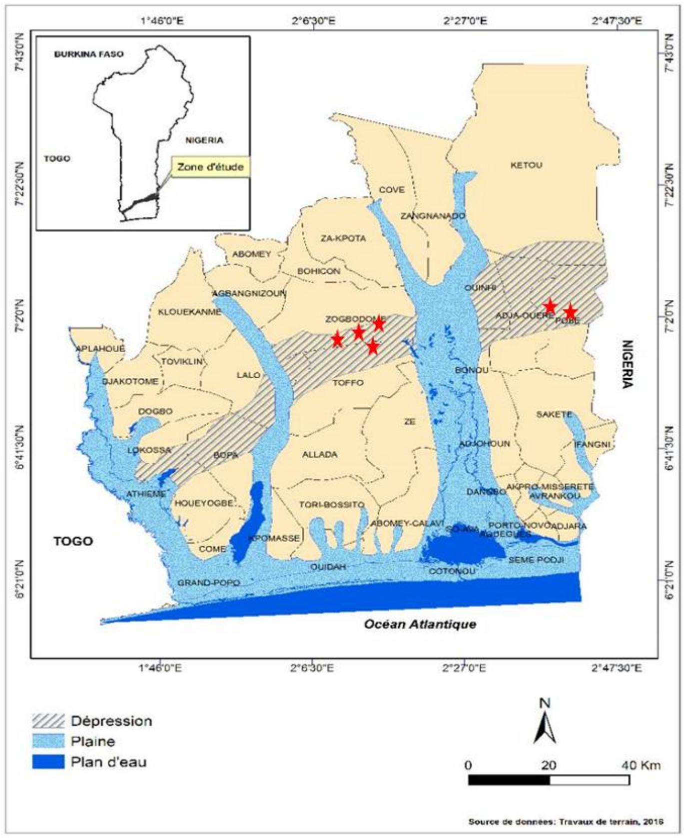

Figure 1. Map of La Lama depression ★ samples locations), Ahlinhan et al., (2025)

Locations	Coordinates	
	Latitude	Longitude
ISSABA	N 07°05’23.8’’	E 02°38’04.9’’
AHOYEYE	N 07°00’33.9’’	E 02°38’04.9’’
SEHOUE MASSI	N 09°44’98’’	E 02°26’31,7’’
ZOUKOU	N 7°02’ 57’’	E 2°10’ 31’’
KOTO	N 6°59’ 57’’	E 2°6’ 43’’
ZOGBODOMEY	N 6°98’48’’	E 2°20’92’’

Table 1. Geolocation of sampling Sites

Disturbed and undisturbed soil samples were collected at a depth of about 3 m with respect to ground level for physical and mechanical tests. Undisturbed samples were extracted using 20 × 20 × 20 cm thin-walled steel boxes driven into the ground, then sealed in plastic bags for transport to the laboratory. The zone of influence for active expansive soils extends from 0 to 2.5 m below ground level, below which moisture content and liquidity index remain nearly constant (Ahlinhan et al., 2025).

Methods

Experimental and numerical methods have been applied. The experimental method involves characterizing the soil through geotechnical tests of its physical and mechanical properties. The detailed experimental procedure is reported in a study of Ahlinhan et al., (2025). In addition, the swelling and shrinkage of expansive clay have been measured in function of cyclic number of wetting-drying. The performance of the expansive clay under cyclic wetting-drying and drying-wetting has been assessed and compared. A three-dimensional finite element model of expansive soil subjected to cyclic drying-wetting beneath a pavement system has been developed by means of the commercial software Abaqus 3D CAE Version. The aim of this numerical model is to analyse the pavement response the soil support consisting of expansive soil subjected to repeated shrink-swell due to environmental conditions. Preliminary analyses were conducted to determine the optimal model geometry and mesh size, ensuring sufficient result accuracy while minimizing the influence of boundary conditions. Based on these analyses, the model was defined with dimensions of 15 m × 15 m in plan and a depth of 10 m. The pavement structure modelled consists of a surface layer of bituminous concrete with 0.07 m thickness, followed by a base layer of laterite gravel with 0.15 m thickness, a sub-base layer of cement treated gravel with 0.20 m thickness, and a subgrade layer of laterite gravel with 0.20 m thickness.

The elastic behaviour is considered for the different layers of the pavement. Table 2 presents the parameters of the properties of the pavement layers. A static load was applied to at the centre of the FE model. This load was applied perpendicularly to equivalent surface of the pavement, approximately corresponding to the footprint of a truck tire (Hadi et al. 2003). The load used in this analysis is 3.25 tons, representing the load on one wheel of a standard 13-ton tandem axle load. Fixed boundary conditions are applied at the corner and bottom of the model. The parallel faces to the z-axis are blocked in the direction of the x-axis, and the model is fixed at the bottom (Wang et al., 2021).

A mesh based on C3D8R (8-node elements with reduced integration) available in the Abaqus 3D has been applied at the loading zone. A coarser mesh of C3D8 elements is used elsewhere to optimise calculation times while maintaining good accuracy. The numerical model was validated through comparison of its results with measured in-situ deflection of Falling Weight Deflectometer (FWD) and the numerical deflection. Hoffman and Thompson (1981, 1982), Han et al., (2021), Wang et al., (2024) found that FWD deflections closely correlate with those from moving wheel loads. The Falling Weight Deflectometer (FWD), which is part of a large family of non-destructive testing (NDT) instruments, was used to measure the pavement deflection in-situ. FWD is designed to monitor the deflection caused by an impact on a circular plate in contact with the pavement surface, with a load corresponding to half the axle load of a lorry moving at a speed of between 50 and 70 km/h, and at the same time to measure the deflections (vertical displacements on the surface) produced on the road surface. The drop height of the mass is variable, and several loads can be obtained, ranging from 20 to 75 KN. The force magnitude is calculated as the product of the falling mass and the impact acceleration. Sensors positioned at the loading center and at specified radial distances from the center measure the resulting surface deflections. The resulting spatial distribution of deflections is referred to as the deflection basin.

Layer	Materials	Thickness (m)	Poisson ratio (-)	Young Modulus (MPa)
Surface	Bituminous concrete	0.08	0.35	500
Base	Gravel (untreated)	0.15	0.35	400
Subbase	Gravel laterite treated with cement	0.20	0.25	1380
Subgrade	Gravel laterite (untreated)	0.20	0.35	400
Soil support	Expansive soil	infinite	-	-

Table 2. Parameters of pavement layers

3. RESULTS AND DISCUSSIONS

Soil Identification

Figure 2 presents the grain-size distribution of the expansive soils gathered in the study area. The soil consists predominantly of high plastic over consolidated silty clay with small fraction of sand. In accordance with the GTR classification, the soils of Issaba are categorized as A4 (highly plastic clays and clay marls). The soil of Ahoyeye belongs to class A3 (clay marls and clays, highly plastic silts). Sehoue-Massi samples are classified as A7-5 according to the Highway Research Board (HRB) classification.

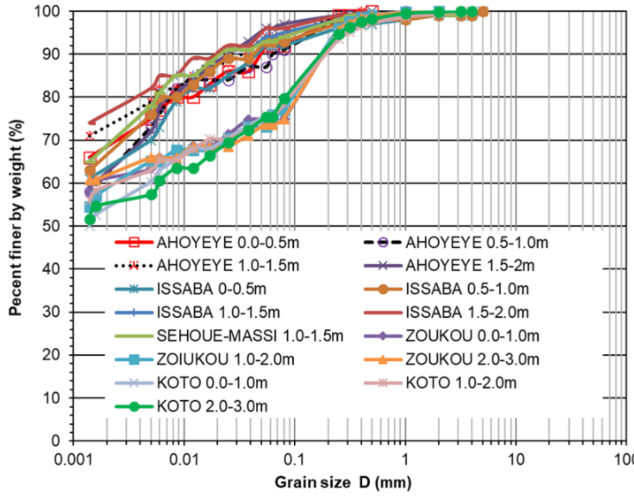

Figure 2. Grading curves of expansive clay

Soil texture variation under cyclic drying-wetting

Samples subjected to alternating shrink-swell cycles exhibited progressive textural changes. Initially (cycle 0), with a natural moisture content of approximately 40%, samples showed minimal visible cracking (Figure 3). Minor swelling occurred after the first wetting phase, followed by cracking and shrinkage during drying phase. This trend continued in subsequent cycles, with swelling and shrinkage intensifying from cycle n–1 to cycle n. The near-complete shrinkage during the drying phase suggests substantial evapotranspiration of free water.

As moisture was lost, clay particles separated from each other, enlarging apparent voids. This increase in pore volume enhances water absorption upon rewetting, thereby raising the potential for compressibility and consolidation. Sample degradation progressed through the second and third cycles, with increasing magnitudes of swelling and shrinkage. Crack geometry (width, length and depth), crack pattern complexity, and brittleness intensified as the number of shrink-swell cycles increased. Consequently, the clay structure deteriorated, consistent with observations by Basma et al., (1993). Similarly, Louati et al., (2021) reported continuous particle reorganization in low-density samples, followed by densification or interaggregate compaction, and an increase in both the number and width of microcracks with successive wetting-drying cycles.

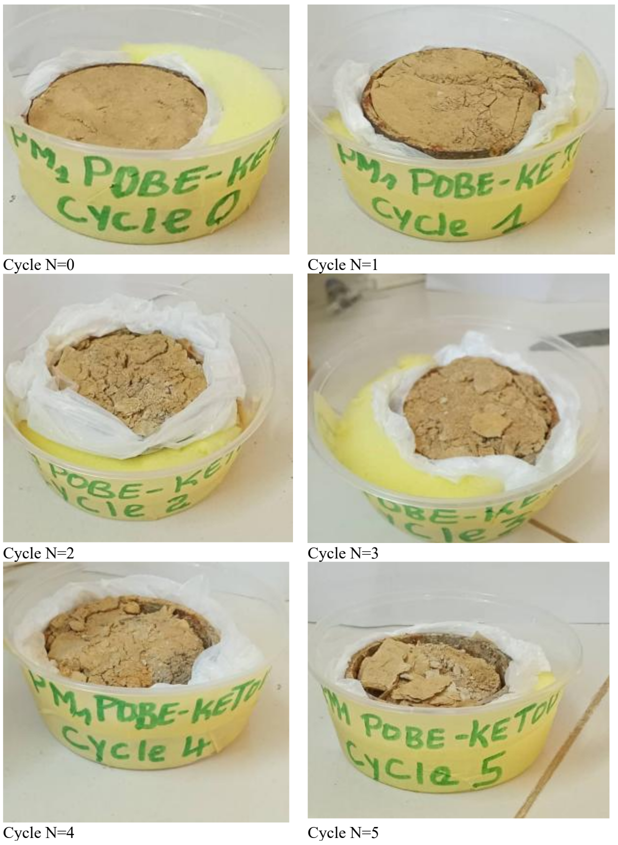

Figure 3. Development for swelling, shrinkage, cracks and mesopores with increasing cyclic alternated drying-swelling, Ahlinhan et al., (2025)

As the number of shrink-swell cycles increases, crack magnitude also increases, leading to a rise in mesopore volume (Figure 3). These mesopores and cracks serve as preferential flow paths, thereby enhancing the soil permeability. This increase in saturated hydraulic conductivity with cyclic wetting and drying has been reported by Shear et al., (1992), Albrecht and Benson (2001), Akcanca and Aytekin (2014), Day (1994, 1997, 1998), Louati et al., (2018), and Azizi et al., (2020). However, a decrease in saturated hydraulic conductivity has been reported for expansive clays subjected to cyclic swell-shrink under constant stress in oedometer tests (Abbas et al., 2023; Albrecht and Benson 2001). This discrepancy is attributed to the clay mineral type, which influences crack self-healing during rewetting. High montmorillonite content can particularly promote healing of cracks formed during drying (Day 1998; Abbas et al. 2023). Furthermore, shrinkage accumulation during cyclic shrink-swell reduces void ratio. Day (1997) observed that continued rewetting enhances clay's expansive properties, aiding in crack healing and reducing hydraulic conductivity. Key factors affecting expansive clay behaviour under repeated drying-wetting include dominant clay mineral, placement conditions (moisture content and dry density), and surcharge level. These findings highlight the progressive structural degradation of expansive soils during shrink-swell cycles.

Expansive soil volume change in cyclic drying-wetting

Figure 4 presents the swelling and shrinkage depending on the number of wetting-drying cycle. The value of shrinkage increases with increasing number of drying-wetting cycle, whereas the value of swelling decreases with increasing number of drying-wetting cycle. The increase of the shrinkage with the number of cyclic drying-wetting can be explained with the increasing number and magnitude of the cracks observed as the number of cyclic wetting-drying increases. Indeed, the cracks of previous cycle favour the shrinkage for the next drying cycle. The measured vertical shrinkage ranges from 11% to 49%, whereas the measured radial shrinking ranges from 11% to 39%.

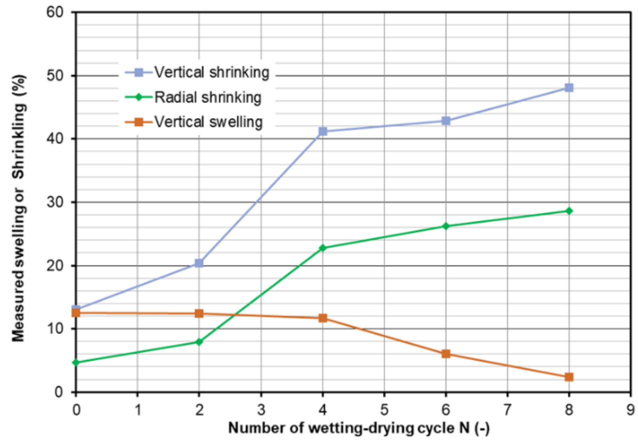

Figure 4. Measured swelling and shrinking with number of wetting-drying cycle

The reduction in swelling of the expansive clay with increasing drying-wetting cycles (Figure 4), can be explained with several interrelated factors that influence its structure and physical properties. Under each cycle, the clay particles undergo rearrangements that strengthen the bonds between them, resulting in compaction of the material. This compaction reduces part of the pore available for expansion, thus limiting the clay's ability to swell during wetting phases. In addition, repeated cycles result in progressive degradation of pore connectivity, making the clay less effective for retaining water. Repeated drying-wetting condition also alters the chemical bonds between particles, reducing their swelling potential. These mechanisms, combined with changes in microstructure, result in a progressive reduction in the swelling capacity of the expansive clay with increasing drying-wetting cycles, affecting its hydromechanical behaviour.

Shear behaviour of expansive soil under cyclic drying-wetting

The shear behaviour of expansive soil under drying-wetting cycles was analysed through direct shear tests. Figure 5 shows the shear stress versus strain for expansive clay under cyclic drying-wetting. The results indicate non-linear behaviour, with a hardening effect in the plastic zone and an increase in shear stress as normal stress (σ_2) rises with the number of cycles.

Shear stress decreases with the number of drying-wetting cycles for a given normal stress (σ_2), with the most significant reduction occurring within the first 3 to 4 cycles. After cycle 4, shear strength stabilizes, indicating equilibrium. The stress-strain curves show no pronounced peaks, reflecting hardening failure rather than brittle behaviour (Figure 5). Moreover, the shear lines drop down as the number of cyclic drying-wetting increases, indicating the drop in the shear strength with the number of cyclic drying-wetting (Figure 6). As a result, the soil fabric mobilizes lower shear strength with increasing cyclic drying-wetting under unconsolidated undrained condition i.e. short-term behaviour of expansive soil. Indeed, the degradation of the soil fabric due to increasing cracks und decreasing swelling potential as the number of alternated cyclic drying-wetting increases (Ahlinhan et al., 2025).

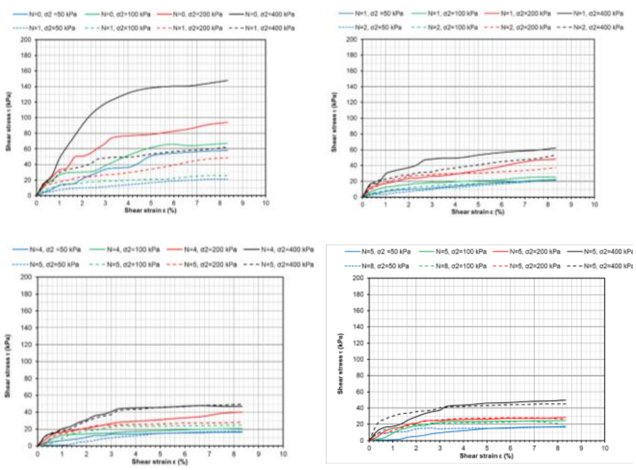

Figure 5. Shear stress depending on shear strain for expansive clay in direct shear test

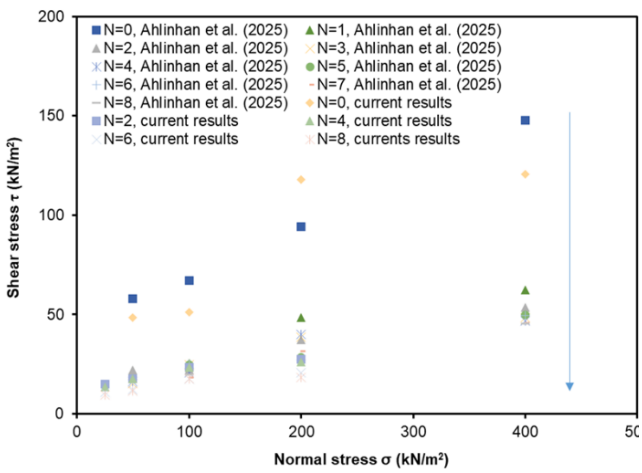

Figure 6. Shear failure envelope for expansive clay in direct shear test

The interaction diagram of the shear strength ($\mathrm{Log}\tau_n/\mathrm{Log}\tau_0$) derived from tests results is presented in Figure 7, which shows that the ($\mathrm{Log}\tau_n/\mathrm{Log}\tau_0$)–N interaction is almost linear. As expected, the overburden pressure and the number of drying-wetting cycle of the soil significantly affect the mobilized shear stress. The larger the number of drying-wetting cycle, the smaller is the shear resistance mobilized. On the other hand, the larger the overburden pressure of the soil, the larger is the shear resistance mobilized.

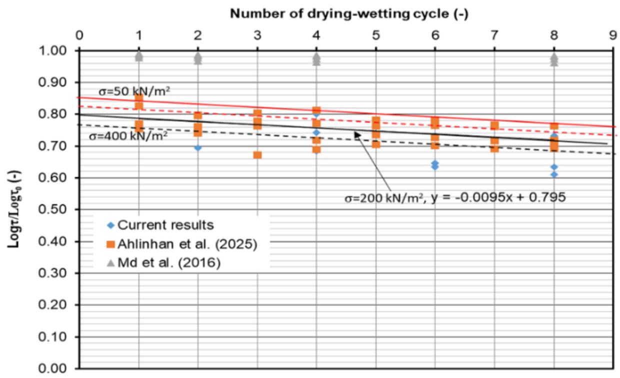

Figure 7. $\mathrm{Log}(\tau_n)/\mathrm{Log}(\tau_0)$ depending on number of drying-wetting cycle

In addition, no clear relation was observed between the normalized shear resistance and the number of drying-wetting cycle, when the shear resistance is normalized as follows: τ_n/τ_0, $\mathrm{Log}(\tau_n/\tau_0)$. Therefore, the general relationship between the resistance of the soil in terms of mobilized shear stress and the number of drying-wetting cycle can be expressed as follows:

$$\tau_N = \tau_0^{(aN+b)} \quad (1)$$

Here, is the τ_N shear stress of the N cycle, τ_0 is the initial shear stress i.e. the shear stress of N=0, a and b are parameters accounting for shear stress degradation as N increases.

Clear trends for the considered four different overburden pressure state (σ=50, 100, 200, 300 and 400 kPa) are obtained (Figure 7). The trend lines for each of the above-mentioned overburden pressure are described by the equations in Table 8.

Overburden pressure (kPa)	Mobilized shear strength (kPa)
$\sigma \leq 50$	$\tau_N = \tau_0^{(-0.0095N+0.845)}$
$50 < \sigma \leq 100$	$\tau_N = \tau_0^{(-0.0095N+0.820)}$
$100 < \sigma \leq 200$	$\tau_N = \tau_0^{(-0.0095N+0.795)}$
$200 < \sigma \leq 400$	$\tau_N = \tau_0^{(-0.0095N+0.760)}$

Table 8. Decrease of mobilized shear strength with overburden pressure and number of cycles

The mobilized shear stresses are dependent of the overburden pressure and are almost linear and parallel to each other for the overburden pressure considered.

Figure 7 presents also a comparison of the results for the mobilized shear stress with those reported by Md et al., (2016). These results show also that the mobilized shear strength decreases with increasing number of drying-wetting cycles. On the other hand, the larger the overburden pressure, the larger is the mobilized shear strength. However, the degradation of the initial shear strength for the expansive clay in the La Lama depression in Benin is significantly larger than that of Kaiping, Gaungdong in China. That can be explained with the test conditions, unconsolidated undrained, consolidated drained condition, the microstructure, and the clay minerals contents of the expansive clay (Ahlinhan et al., 2025).

The dependence of the undrained angle of internal friction and the undrained cohesion on the repeated drying-wetting is presented in Figure 9 and Figure 10, respectively. For the current results, two types of the tests were carried out on the expansive clay gathered along the road section POBE-KETOU. The type W-D, i.e. the samples were first wetted and then dried, so that the shear tests were performed on dried samples. The type D-W, i.e. the samples were first dried and wetted then, so that the shear tests were performed on dried samples. As expected, the undrained angle of internal friction and the undrained cohesion for the type D-W are larger than those for the type W-D due to large excess pore pressure in the case of type D-W.

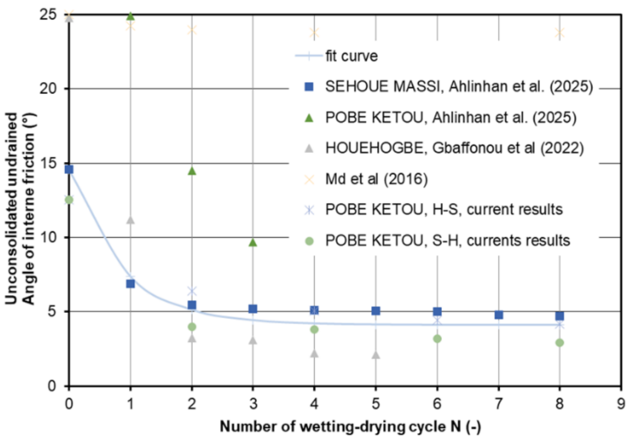

Figure 9. Dependence of undrained angle of internal fiction with cycle number

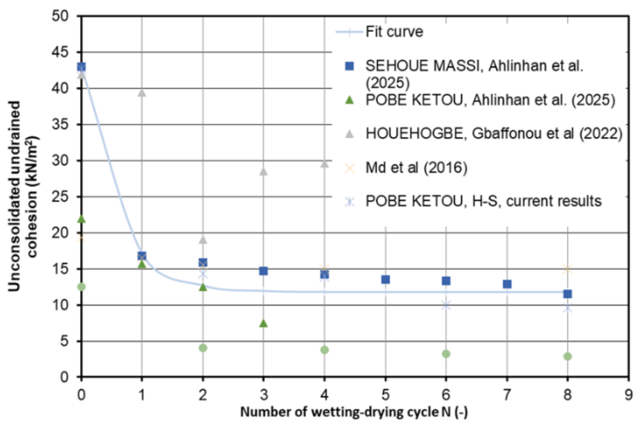

Figure 10. Dependence of undrained cohesion with cycle number

The angle of internal friction and the cohesion decrease with increasing number of cyclic alternated drying-wetting. Most significant decay is noted for the first and second cycle, above which both the undrained angle of internal friction and the undrained cohesion remain almost constant, indicating the equilibrium state is reached for the samples of expansive clay.

$$\varphi_{uu} = 10.45 \cdot e^{-1.16 \cdot N} + 4.11 \tag{2}$$

$$c_{uu} = 31.11 \cdot e^{-1.77 \cdot N} + 11.81 \tag{3}$$

The undrained angle of internal friction was decreased significantly for first two cycles for reaching a residual angle of internal friction ranging from 20% to 30% of the initial angle of internal friction (Figure 9). For the samples tested this residual angle of internal friction is approximately 5°, indicating that an equilibrium state is reached. The unconsolidated undrained angle of internal friction φ_{uu} for the expansive soil tested can expressed in function of the number of cyclic drying-wetting N with the equation 1.

Likewise, the undrained cohesion was decreased significantly for first two cycles for reaching a residual undrained cohesion approximately 35% of the initial undrained cohesion (Figure 10). For the samples tested this residual undrained cohesion ranging from 10 to 15 kPa, indicating that an equilibrium state is reached. The unconsolidated undrained cohesion c_{uu} for the expansive soils tested can be expressed in function of the number of cyclic drying-wetting N by the equation 2. According to equation 1 and 2, the degradation factor is 1.16 and 1.77 for the angle of internal friction and the cohesion, respectively. That confirms, the findings that the degradation of the cohesion is larger than that of the angle of internal friction (Ahlinhan et al., 2025; Md et al. 2016).

These results are consistent with degradation of the internal friction angle and the cohesion reported by Gbaffonou et al., (2021), Gbaffonou (2022) for expansive soil in direct shear test in the city of Houehogbe in the la Lama depression (Ahlinhan et al. 2025). The results of residual cohesion are comparable with those reported by Md et al., (2016). However, Md et al., (2016) observed attenuation to 95% of the initial internal angle of friction and 80% of the initial cohesion for expansive soil of Kaiping, Gaungdong in China under the cyclic swell-shrink triaxial shear tests in consolidated drained condition. This discrepancy in degradation percent can be explained with the test conditions, unconsolidated undrained, consolidated drained condition, the microstructure, and the clay minerals contents of the expansive clay. Indeed, montmorillonite like minerals experience significant degradation in comparison to kaolinite and illite like minerals due the T-O-T microstructure of the montmorillonite and the resulting high activity (Ahlinhan et al., 2025). The undrained shear strength of the expansive soils investigated decreases significantly from 0 to 2 cycles of alternating shrinkage-swell. Therefore, lightly loaded structures, i.e. light buildings, railways and pavements on expansive soils, will be subject to reduced bearing capacity and differential settlement from the second cycle onwards, potentially leading to premature cracking and damage. This can justify the cracking and damages often observed 2 years after the construction and commissioning of civil infrastructure on expansive clay in the La Lama depression.

Compressibility and consolidation behaviour under cyclic drying-wetting

The compressibility and the consolidation response of expansive soils under cyclic drying-wetting was analysed by means of the oedometer tests. The test results showed an almost linear increase in the void ratio as the number of cyclic drying-wetting cycle increases (Figure 11). Although, the samples of expansive clay gathered from SEHOUE-MASSI and POBE-KETOU present a comparable initial void ratio, the increase in void ratio for expansive from SEHOUE-MASSI is more significant than that from POBE-KETOU. The increase in void ratio between two successive drying-wetting cycles ranges from 6% to 30%. This increase in void ratio can be explained by the increasing development of cracks observed in the soil samples, and therefore the increase in macropores with increasing number of alternating dry-wet cycles.

The oedometer test results in terms of the compressibility, as depicted in Figure 12, show an increase in the void ratio with the increasing cyclic drying-wetting, and a decrease in the void ratio with the overburden pressure. The results were consistent with the increase of the hydraulic conductivity with increasing cyclic wetting-drying (Shear et al., 1992; Albrecht and Benson 2001; Akcanca and Aytekin 2014; Day 1998; Louati et al., 2018; Azizi et al., 2020; Day 1997). The increase of the void ratio with increasing drying-wetting can be explained with the observed macropores due to the cracking of the soil sample under drying condition.

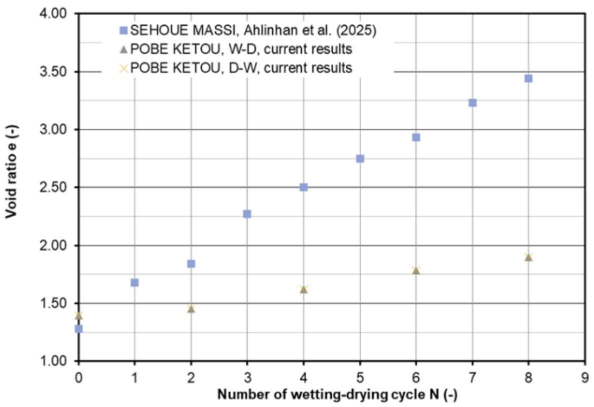

Figure 11. Increase of void ratio with increasing number of cyclic wetting-drying

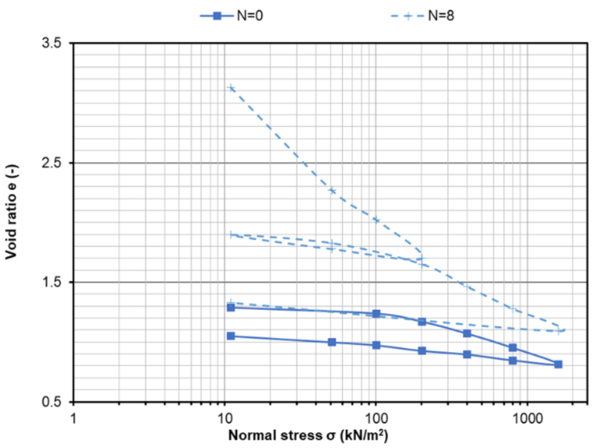

Figure 12. Void ratio with normal stress for N=0, N=8

Figure 13 illustrates the evolution of the swelling index with the number of cycles. The swelling index decreases as the number of drying-wetting cycles increases, indicating a growing tendency of the soil to contract in volume. Although the expansive soil exhibits reduced swelling potential compared to its initial state, this decrease appears to stabilize after the fourth cycle. This behaviour may be attributed to the breakdown of soil aggregates and the formation of new macropores and/or micropores. These findings align with those of Gbaffonou et al., (2022); Soltani et al., (2022); Dif and Bluemel (1991); Al-Homoud et al., (1995); Basma et al., (1996); Tripathy et al. (2002); Estabragh et al. (2015), who reported that swelling potential decreases with repeated drying-wetting cycles until it stabilizes.

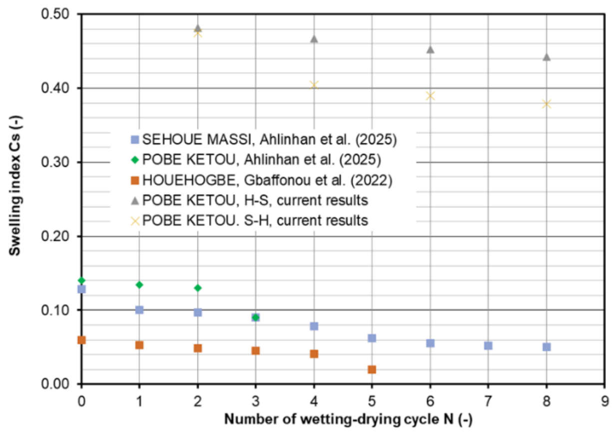

Figure 13. Evolution of swelling index Cs with number of cyclic wetting-drying

This behaviour may result from the ongoing rearrangement of soil particles. However, studies by Popescu (1979), Osipov et al., (1987) and Day (1994) observed the opposite trend: an increase in swelling with more cycles. This discrepancy likely depends on the soil's geological origin, clay mineralogy, and stress conditions.

Figure 14 delineates the evolution of the constrained or oedometer modulus as the number of cyclic drying-wetting increases. There's an increase in the constrained modulus with increasing cyclic drying-wetting, indicating hardening and stiffer response of the soil. The increase in constrained modulus between two consecutive cycles of drying-wetting ranges from 3% to 7%. This increase in constrained modulus could be attributed to the initial densification due to rearrangement of soil particles. This result is consistent with the findings reported by Liu et al. (2020). However, the soils of Houehogbe showed an increase in constrained from the first to second cycle, thereafter a decrease in constrained modulus (Gbaffonou et al., 2022). This softening behaviour could be attributed to the progressive breakdown of soil structures or the weakening of bonds between particles due to repeated drying-wetting.

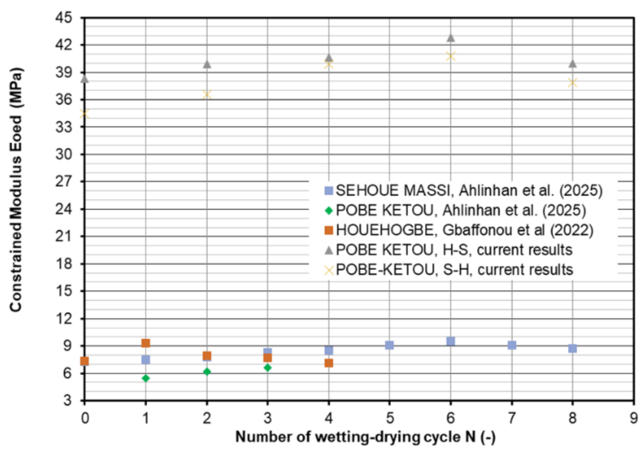

Figure 14. Evolution of oedometer modulus with number of cyclic drying-wetting

Table 15 summarizes the soil parameters obtained from experimental tests carried out on expansive soil subjected to repeated drying-wetting.

Number of Cycle N	0	2	4	6	8
Depth / Properties	1.5m-2m	1.5m-2m	1.5m-2m	1.5m-2m	1.5m-2m
Unit weight satured (kN/m^3)	17.08	16.70	16.94	17.25	17.28
Unit weight unsatured (kN/m^3)	11.27	11.17	11.60	12.27	12.57
Constrained modulus (MPa)	34.45	36.60	39.90	40.75	37.90
Young modulus (MPa)	23.25	24.71	26.92	27.50	25.58
Poisson ratio v	0.35	0.35	0.35	0.35	0.35
Cu (kPa)	42.78	14.34	13.91	10	9.60
φ_u (°)	12.53	4.01	3.80	3.20	2.90

Table 15. Soil properties depending on number of cycles of shrink-swell

FE results

Figure 16 presents the finite element model, which measures 15 meters in width and length, and 10 meters in depth. The model consists of several layers: a surface layer with tyre twinning (black mesh), followed by a base layer (blue mesh), a subbase layer (red mesh), a subgrade layer (white mesh), and finally the expansive soil layer (orange mesh). For the validation of the numerical model, back-calculations of the fall deflector tests on pavement have been carried out. Furthermore, an additional back-calculation by means of the pavement design code Alizé has been carried out.

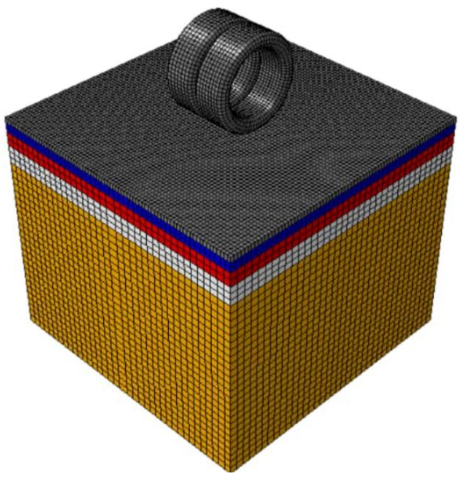

Figure 16. Model mesh

In situ pavement deflection measured by means of falling weight deflectometer test were evaluated and compared with the numerical analysis results (Figure 17). As expected, the displacement of the pavement structure is maximum around the footprint of the tyres, and decreases with increasing distance from the tyre's footprint. It was found that both numerical results fall in the range of the in-situ FWD results. The measured and numerical deflections are very comparable; hence the FE Model is validated. The validated model was used to perform parametric study. For that, the test results on expansive soils presented in section from 4.1 to 4.6, and summarized in Table 15 have been applied.

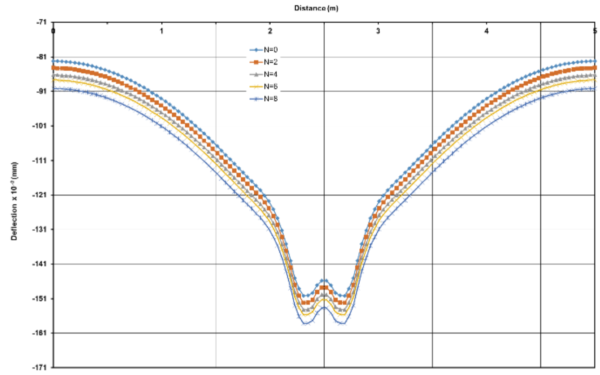

Figure 17. Pavement deflection

The cross-section of the vertical displacement for the number of cyclic drying-wetting N=0 through the tyre footprint is presented in Figure 18.

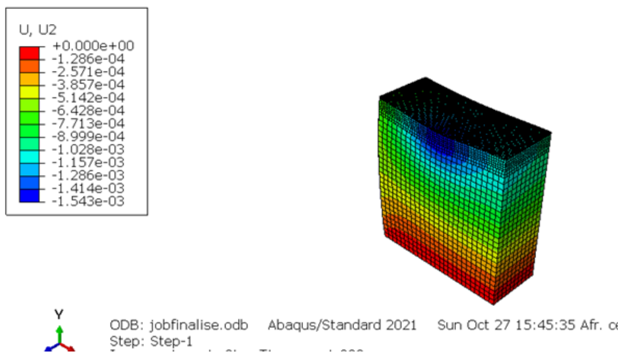

Figure 18. Displacement for number of cycle N=0 under traffic load

The settlement depression (blue) around the tyre footprint highlighted a maximum settlement of $1.53\cdot10^{-3}$ m. Figure 19 presents the pavement deflection depending on the number of cyclic drying-wetting. As expected, the displacement is maximum around the footprint of the tyres and decreases with increasing distance from the tyre's footprint. The pavement deflection increases as the number of cyclic drying-wetting increases. Each additional cycle causes an increase in vertical displacement of about 1 mm/100. The vertical displacement was maximum under the tyre foot print, then decreases with increasing distance from the foot print.

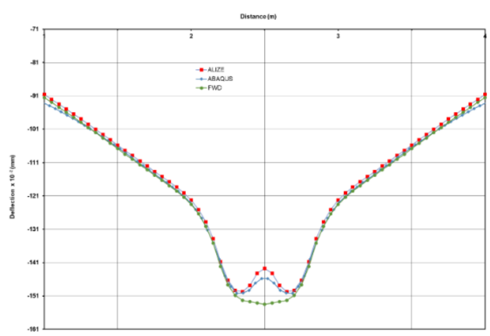

Figure 19. Comparison between in-situ and numerical deflection

Figure 20 highlights a phenomenon of shear strain stabilisation with increasing shrink-swell cycles. It appears that each additional cycle causes an increase in deformation of about 5 mm/100. However, from the sixth cycle onwards, the shear strain tends to stabilise, indicating a reduction in the variability of the clay's mechanical behaviour due to moisture variations.

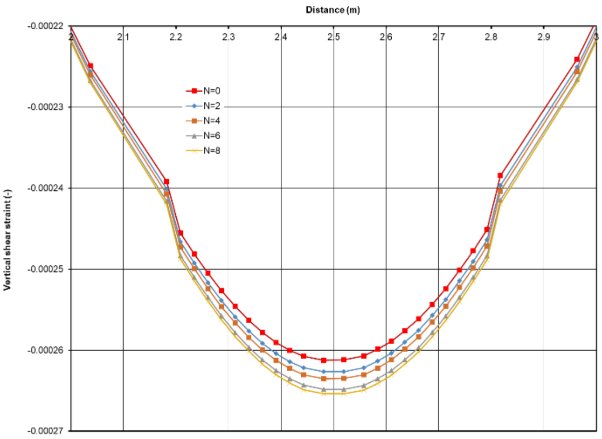

Figure 20. Vertical shear strain of pavement at surface of support platform as a function of cycle

This gradual stabilisation of the shear strain can be explained with a reorganisation of the soil microstructure under repeated shrink-swell, leading to a state of equilibrium. This behaviour is typical for expansive clay soils.

4. CONCLUSIONS

This study presents the effects of alternated drying-wetting cycles on the performance of expansive soil. For that, series of oedometer and direct shear tests have been performed, and saturated undrained angle of internal friction, cohesion, swelling, shrinkage, swelling index and constrained modulus were assessed in function of the number of repeated drying-wetting. The cyclic alternated drying-wetting and the corresponding shrink-swell leads to the rearrangement of soil fabric, as a result the unconsolidated undrained angle of internal friction and cohesion decrease with increasing repeated drying-wetting. This can be explained with the degradation or the reduction of the physico-mechanical and or microstructural properties of the expansive clay as the number of cycles increases.

The expansive soil subjected to cyclic alternated drying-wetting showed that the magnitude of the cracks and mesopores increases with increasing cyclic drying-wetting. The soil fabric becomes more brittle with increasing cyclic wetting-drying so that the degradation of the soil fabric can be stated.

The results of the direct shear tests showed that the unconsolidated undrained shear strength (angle of internal friction and cohesion) decreases as the number of cycles increases. The unconsolidated undrained angle of internal friction decreased to 30% of the initial angle of internal friction, while the unconsolidated undrained cohesion decreases to 35% initial cohesion. Hereby, the most degradation occurs for a number of cycles of approximately 2, above the equilibrium is reached. The derived normalized interaction diagrams and equations relating the shear resistance, the angle of internal friction and the cohesion to the number of cycles constitute an adequate tool for the preliminary design.

Moreover, consolidation tests were performed out to analyse the compressibility and the consolidation behaviour of expansive soils. The results of the oedometer tests showed a decrease of the swelling index with the number of cycles, implying a greater propensity of the soil to undergo volume contraction when exposed to cyclic wetting-drying. The value of shrinkage increases with increasing number of wetting-drying cycle, whereas the value of swelling decreases with increasing number of wetting-drying cycle.

Furthermore, three-dimensional FE analyses were performed to investigate the response of pavement resting on expansive clay subjected to repeated drying-wetting. The constitutive law of Mohr Coulomb (MC) that captures the elastoplastic behaviour of soil was applied. The numerical model was calibrated using the results from falling weight deflectometer. The following main conclusions can be drawn from the FE results obtained:

- Back-calculation of falling weight deflectometer showed that the response of pavement under loading conditions can be adequately predicted by means of a numerical model using the Mohr Coulomb (MC) law.
- Pavement deflection and shear strain increase as the number of cycles increases. The displacement is maximum around the footprint of the tyres and decreases with increasing distance from the tyre's footprint.
- Value of the shear strain tends to be stabilized as the number of repeated drying-wetting increases.

These findings show that repeated shrink-swell induces progressive deterioration of interparticle contacts within the expansive clay matrix. Concurrently, it facilitates the reconfiguration, reorganisation, and reorientation of large micro-aggregates through the disorientation of structural components. These microstructural transformations collectively result in a progressive modification of the shrink-swell behaviour in terms of the shear resistance, the compressibility and the consolidation as the number of drying-wetting cycles increases.

References

M.F. Ahlinhan, O. J. Dansou, B. D. Djenou, L. Sounouvou, E. C. Adjovi. 2025. "Swelling and Shrinkage Performance of Expansive Soils under Repeated Moisture Variations". Current Journal of Applied Science and Technology 44 (4):91-110. https://doi.org/10.9734/cjast/2025/v44i44517.

E. Chabi, O. G. Adéoti, M. F. Ahlinhan, M. L. Agassoussi (2025). Evaluating pavement performance on expansive clay soils subjected to cyclic shrinkage and swelling. Open Journal of Applied Sciences, 15(1), 70-97.

S.H. Md, K. Ling-wei, Y. Song, Effect of drying-wetting cycles on saturated shear strength of undisturbed residual soils, American Journal of Civil Engineering. 4 (2016) 143–150.

A.A. Basma, A.S. Al-Homoud, A.I.H. Malkawi, M.A. Al-Bashabsheh, Swelling-shrinkage behavior of natural expansive clays, Applied Clay Science. 11 (1996) 211–227.

F. Louati, H. Trabelsi, M. Jamei, S. Taibi, Impact of wetting-drying cycles and cracks on the permeability of compacted clayey soil, European Journal of Environmental and Civil Engineering. 25 (2018) 696–721.

B. Gbaffonou, Y. Tankpinou Kiki, V. Tohoungba, V.S. Gbaguidi, Influence of drying-wetting cycles on the compressibility of clay soils in the commune of Houeyogbe, IJESRT. 10 (2021) 11. https://doi.org/10.29121/ijesrt.v10.i5.2021.1.

B. Gbaffonou, Influence des cycles de séchage-humidification sur les paramètres mécaniques des sols argileux : Cas de la commune de Houéyogbé (2022), Thèse de doctorat de l´université d´Abomey-Calavi.

Abbas, M.F., Shakerc, AA, Al-Shamrani, M,A, (2023) Hydraulic and volume change behaviors of compacted highly expansive soil under cyclic wetting and drying Journal of Rock Mechanics and Geotechnical Engineering 15, 486-499.

NF EN ISO 17892-1 Reconnaissance et essais géotechniques - Essais de laboratoire sur les sols - Partie 1 : détermination de la teneur en eau, Association Française de Normalisation. (2014).

NF EN ISO 17892-12 Reconnaissance et essais géotechniques - Essais de laboratoire sur les sols - Partie 12 : détermination des limites de liquidité et de plasticité, Association Française de Normalisation. (2018).

NF EN ISO 17892-3 Reconnaissance et essais géotechniques - Essais de laboratoire sur les sols - Partie 3 : détermination de la masse volumique des particules solides, Association Française de Normalisation. (2015).

ISO 14235 Soil quality — Determination of organic carbon by sulfochromic oxidation, International Standard Organization (1998).

NF EN ISO 17892-4 Reconnaissance et essais géotechniques - Essais de laboratoire sur les sols - Partie 4 : Détermination de la distribution granulométrie des particules, Association Française de Normalisation. (2018).

NF EN ISO 17892-5 Reconnaissance et essais géotechniques - Essais de laboratoire sur les sols - Partie 5 : Essai de chargement par palier à l'œdomètre, Association Française de Normalisation. (2017).

NF EN ISO 17892-10 Reconnaissance et essais géotechniques - Essais de laboratoire des sols - Partie 10 : Essai de cisaillement direct, Association Française de Normalisation. (2018).

Tankpinou Kiki S.T. (2016) Caractérisation minéralogique, thermique er microscopique des sols fins en technique routièr. Thése de doctorat de l´université d´Abomey-Calavi et de l´université de Bordeaux.

Shear, D., Olsen, H., Nelson, K., 1992. Effects of desiccation on the hydraulic conductivity versus void ratio relationship for a natural clay. Transport. Res. Rec. 1369, 130-135.

Albrecht, B.A., Benson, C.H., 2001. Effect of desiccation on compacted natural clays. J. Geotech. Geoenviron. Eng. 127, 67-75.

Akcanca, F., Aytekin, M., 2014. Impact of wetting-drying cycles on the hydraulic conductivity of liners made of lime-stabilized sand-bentonite mixtures for sanitary landfills. Environ. Earth Sci. 72, 59-66.

Day, R.W., 1994. Swell-shrink behavior of compacted clay. J. Geotech. Geoenviron. Eng. ASCE 120, 618-623.

Day, R.W.,1997. Discussion of hydraulic conductivity of desiccated geosynthetic clay liners. J. Geotech. Geoenviron. Eng. 123, 484-486.

Day, R.W., 1998. Discussion: infiltration tests on fractured compacted clay. J. Geotech. Geoenviron. Eng. 124, 1149-1152.

Azizi, A., Musso, G., Jommi, C., 2020. Effects of repeated hydraulic loads on microstructure and hydraulic behaviour of a compacted clayeysilt. Can. Geotech. J. 57, 100-114.

Soltani A, Raeesi R and O'Kelly BC (2022) Cyclic swell–shrink behaviour of an expansive soil treated with a sulfonated oil. Proceedings of the Institution of Civil Engineers – Ground Improvement 175(3): 166–179, https://doi.org/10.1680/jgrim.19.00084.

Dif, A., Bluemel, W., 1991. Expansive soils under cyclic drying and wetting. Geotech.Test J. 14, 96-102.

Al-Homoud, A.S., Basma, A.A., Husein Malkawi, A.I., Al Bashabsheh, M.A., 1995. Cyclic swelling behavior of clays. J. Geotech. Eng. 121, 562-565.

Tripathy, S., Rao, K.S., Fredlund, D.G., 2002. Water content void ratio swell-shrink paths of compacted expansive soils. Can. Geotech. J. 39, 938-959.

Estabragh A.R., Parsaei J.B., Javadi A.A., (2015) Laboratory investigation of the effect of cyclic wetting and drying on the behaviour of an expansive soil. Soils and Foundations, 2015; 55 (2): 304-314.

Popescu, M.E., 1980. Behaviour of expansive soils with crumb structures. In: Proceedings of the 4th International Conference on Expansive Soils, 158-171.

Osipov, V.I., Bik, N.N., Rumjantseva, N.A., 1987. Cyclic swelling of clays. Appl. Clay Sci. 2, 363-374.

Sorensen K.K., Okkels N. (2013) Correlation between drained shear strength and plasticity index of undisturbed overconsolidated clays. In Proceedings of the 18th International Conference on Soil Mechanics and Geotechnical Engineering, Paris, France.

X. Qin, D.-H. Han, L. Zhao. (2019) Elastic characteristics of overpressure due to smectite-to-illite transition based on micromechanism analysis, geophysics, vol. 84, No. 4.

P. Liu; R.-P. Chen, K. Wu, X. Kang (2020) Effects of drying-wetting cycles on the mechanical behavior of reconstituted granite-residual soils, J. Mater. Civ. Eng., 2020, 32(8): 04020199.

Day, R.W., 1999. Geotechnical and Foundation Engineering Design and Construction. McGraw-Hill, New York.

Haines, W.B., 1923. The volume changes associated with variations of water content in soil. J. Agric. Sci. 13, 296-310.

Bell, F.G., 2000. Engineering properties of soils and rocks. Butterwerth Heinemann Ltd., Woburn, MA.

Popescu, M.E., 1979. Engineering problems associated with expansive clays from Romanian. Eng. Geol. 14, 43-53.

Gourley, C. S., Newill, D., Schreiner, H. D. (1994). Expansive soils: TRL's research strategy. In P. G. Fookes & R. H. G. Parry (Eds.), Proceedings of the 1st International Symposium on Engineering Characteristics of Arid Soils (pp. 247 260). Rotterdam: A.A. Balkema. ISBN 9054103655.

A. R. Estabragh, A. Soltani, A. A. Javadi (2018) Effect of pore water chemistry on the behaviour of a kaolin–bentonite mixture during drying and wetting cycles. European Journal of Environmental and Civil Engineering, Volume 24, 2020 - Issue 7, 895-914, https://doi.org/10.1080/19648189.2018.1428691.

Gourley, C. S., Newill, D., & Schreiner, H. D. (1994). Expansive soils: TRL's research strategy. In P. G. Fookes & R. H. G. Parry (Eds.), Proceedings of the 1st International Symposium on Engineering Characteristics of Arid Soils (pp. 247-260). Rotterdam: A.A. Balkema. ISBN 9054103655.

Driscoll, R. M. C., & Crilly, M. S. (2000). Subsidence damage to domestic buildings: Lessons learned and questions remaining (1st Ed.). Watford: CRC Press. ISBN 1860814336.

Chen, F. H. (1975). Foundations on expansive soils (1st Ed.). Amsterdam: Elsevier Scientific Publication Co. ISBN 0444413936.

Nelson, J. D., Miller, D. J. (1992). Expansive soils: Problems and practice in foundation and pavement engineering (1st Ed.). New York: John Wiley & Sons. ISBN 0471511862.

M.S. Hoffman, M.R. Thompson (1981) Nondestructive Testing of Flexible Pavements: Field Testing Program Summary. Transportation Engineering Series 31, Illinois Cooperative highway and Transportation Research Program, Series 188, University of Illinois at Urbana-Champaign.

M.S. Hoffman, M.R. Thompson (1982) Comparative Study of Selected Nondestructive Testing Devices. In Transportation Research Record 852, TRB, National Research Council, Washington, D.C., 1982, pp. 32-41.

1. Han Z., Zhang J., Xue L., Fang H., Xiao Z. Dynamic Simulation of FWD Tests on Flexible Transversely Isotropic Pavements with Imperfect Interfaces. Computers and Geotechnics, Vol. 130, 2021, p. 103914.

Y. Wang, Y. Zhao, F. Wu, Q. Sun (2024) Intelligent Back-calculation Approach to Obtain Viscoelastic Properties of Asphalt Pavements on Bedrock using Falling Weight Deflectometer Tests. Transportation Research Record: Journal of the Transportation Research Board. https://doi.org/10.1177/0361198124129258.